JOURNAL OF MATERIALS SCIENCE 29 (1994) 714–720

Various aspects of the air oxidation behaviour of a Ti6Al4V alloy at temperatures in the range 600–700 °C

S. FRANGINI, A. MIGNONE
Corrosion Laboratory, ENEA CRE Casaccia, CP 2400, 00100 Rome, Italy
F. DE RICCARDIS
Division of Materials, CNRSM, 72100 Brindisi, Italy

A study on the air oxidation behaviour of a commercially pure Ti6Al4V alloy between 600 and 700 °C is reported, based on determination of the kinetic curves, microhardness profiles in the metal beneath the scale, and examination of morphology and composition of the scales. The oxidation kinetics shows a gradual transformation dependent on both time and temperature from a diffusive to a nearly linear rate law. It has been observed that such transformation may be associated with the acceleration of oxide scale growth. This phenomenon is accompanied by a parallel change of the oxide morphology, which is essentially manifested with the onset of a duplex-type scale starting from 650 °C. Aluminium is found to pile up near the external surface of the oxide scales, although the presence of a continuous film of alumina may be excluded under any circumstances. Finally, the effect of aluminium and vanadium is beneficial in reducing appreciably the amount of oxygen dissolved in the surface metal layer, compared with unalloyed titanium.

1. Introduction

Among the high-temperature materials, the titanium-base alloys containing aluminium find satisfactory applications where the requirements of both high strength-to-density ratio and a good oxidation resistance are of primary importance. In recent years a great deal of work has been concerned with design and development of titanium aluminium intermetallic compounds offering significant improvements over the conventional Ti–Al alloys [1–3]. However, their limited ductility at room temperature has represented, until now, a major obstacle in finding adequate fabrication practices, thereby preventing their wider utilization. For these reasons, conventional Ti–Al alloys continue to be largely attractive for airframe applications as well as for low- and medium-temperature sections of aero gas turbine engines. It is well established that problems with creep strength [4] limit the useful service temperature of these alloys at about 550–600 °C. When using them at higher temperatures their ductility can be further compromised through the dissolution of large amounts of oxygen in the metal lattice or the precipitation of intermetallic phases.

Numerous publications have dealt with the high-temperature performances in air or in pure oxygen of binary Ti–Al alloys containing up to a few per cent of aluminium [5–13]. In general, it has been observed that the addition of aluminium reduces oxidation rates, although alloys with less than a critical content are reported to oxidize faster than pure titanium [12]. Most of these studies have discussed the effects of the aluminium content in terms of morphology and composition of the scale [8, 9]. The embrittlement of the metal surface layers promoted by oxygen penetration and its adverse influence on both mechanical and adherence properties of the oxide/metal systems, have also been documented [11, 14].

Therefore, the aim of the present work was mainly to cover the study of these various aspects, presenting some experimental results for air oxidation of the ternary Ti6Al4V alloy after isothermal tests at temperatures in the range 600–700 °C.

This study is part of a larger research programme devoted to providing fundamental information on the oxidation characteristics of Ti–Al intermetallic compounds.

2. Experimental procedure

A commercial, pure Ti6Al4V alloy was examined. The X-ray microanalysis gave the composition of the alloying elements as follows: 88.9 Ti, 6.3 Al, 4.9 V (wt %). The alloy was received in the dual-annealed condition in the form of 15 mm diameter rod. The microstructure consisted typically of small grains of transformed-beta at the triple points of alpha grain boundaries.

Cylindrical coupons, 10 mm diameter and 10 mm high, were cut from the rod, polished with 600 grit SiC

0022–2461 © *1994 Chapman & Hall*

paper and cleaned in a mixture of acetone and toluene prior to oxidation. Isothermal oxidation was carried out by placing each coupon in a horizontal, electrically heated tube furnace. Both the specimen holder and furnace tube were made of recrystallized alumina. The system was heated to the test temperature in about 2 h under a slow argon flow. Once the test temperature was reached, the argon flow was stopped and air was added to the system for the duration of the test. After each test, the furnace was switched off and a slow cooling was carried out in flowing argon in order to minimize scale spalling. The gas flow rates were set at about $1\,l\,h^{-1}$ (about one volume change per hour for the present system) by means of floating-ball flow meters. In order to keep the moisture content of the gases at levels below 1 p.p.m., the gases were passed through a tube containing molecular sieves type Linde-5A before entering the furnace. The temperatures used in this study were in the range 600–700 °C at a total pressure of 1 bar.

The corrosion kinetics were determined by weighing the coupons after 50, 100, 150, 200 and 300 h testing time on a Mettler analytical balance sensitive to ± 0.1 mg. Following oxidation, transverse sections of selected coupons were prepared for metallographic studies and for microhardness measurements. Particular care was given to the specimen mounting technique to avoid pluck of the scales during polishing. After cold mounting in bakelite, the specimens were cut with a diamond wheel and ground with SiC paper smeared with paraffin from 400 to 1000 grades. Subsequently, they were polished using napless cloths impregnated with an aqueous paste of MgO. Finally, they were sputter-coated with carbon to make them suitable for microscopic observations.

Optical microscopy and scanning electron microscopy equipped with an energy dispersive X-ray analyser (SEM + EDX) were used for morphological and compositional studies of the scales. The oxidized phases were identified by performing X-ray diffraction analysis (XRD) on powdered scales using the Debye–Scherrer technique and a cobalt target.

Microhardness profiles in the alloy substrate below the oxide scale were carried out using a Reichert–Jung microhardness tester equipped with a Vickers indentor. The applied load was 0.1 N (10 gf). In order to sample only the alpha phase the coupons were preliminarily etched with the Kroll's reagent that revealed the beta phase.

3. Results

3.1. Oxidation kinetics

The weight gain data obtained after exposure to air of the Ti6Al4V alloy at temperatures of 600, 650 and 700 °C are shown in Fig. 1 together with the corresponding interpolating curves. The scatter bands associated with these curves are in the order of $\pm 10\%$. By fitting the data to an equation of the form $(\Delta W)^n = kt$, it is found that the value of n falls progressively from a nearly cubic to a linear kinetics with increasing temperature (Table I). Moreover, at 700 °C, the transition from diffusive to linear rate law was seen to depend on time so that a unique value of n was considered inadequate to describe satisfactorily the behaviour at both short and long times. This time dependence was not clearly detected at the lower temperatures, presumably owing to the too low exposure lengths of the oxidation tests.

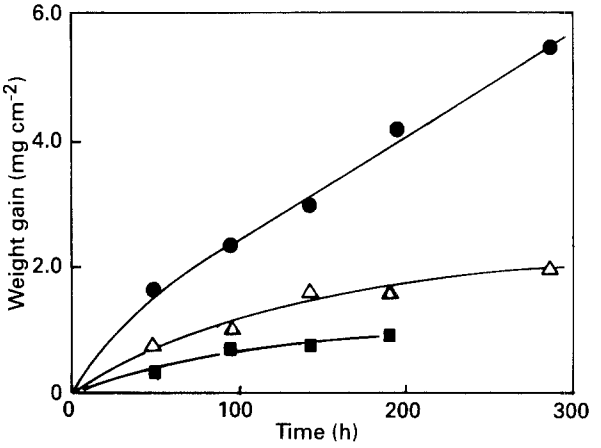

Figure 1 Weight gain of Ti6Al4V during oxidation in air at: (■) 600 °C, (△) 650 °C and (●) 700 °C.

TABLE I Rate exponents, n and parabolic rate constants, k_p, for oxidation in air of Ti6Al4V

T (°C)	n	k_p ($10^4 mg^2 cm^{-4} h^{-1}$)
600	2.8	43
650	1.8	153
700	1.8 ($\leq$ 150 h)	625
	1.2 ($>$ 50 h)	–

Because only the parabolic rate constants, k_p, have a well-established theoretical significance, and to make comparisons possible with other data in the literature, the values of k_p during the protective stages of oxidation were calculated by regression lines that fit a parabolic model of oxidation. At 700 °C, k_p was calculated on the basis of the first 150 h exposure.

Table I gives the corresponding values of k_p, which were used for the determination of the activation energy. A least square line through the experimental data gave a value of about 192 kJ mol^{-1}, which is of comparable magnitude to that reported for unalloyed titanium [9]. It should be noted that the values in Table I have been calculated on the basis of the total weight gain, which means that the amounts of oxygen dissolved in the metal lattice are also included. With the aid of both SEM and light microscopy, measurements of the mean scale thickness at the various temperature/time conditions were determined in order that reaction kinetics for both scale growth and oxygen solution could be calculated. The film thickness was found to be relatively uniform, although occasionally some marked differences existed between flat and curved surfaces of the specimens.

The weight of oxygen in the scales was determined, assuming the density of rutile to be 4.26. The mean error in the determination of film thickness was about ± 1 μm that corresponds to ± 0.15 mg cm^{-2} oxide weight. The knowledge of the total oxygen absorption

TABLE II Comparison of the parabolic rate constants corresponding, respectively, to the kinetics of total oxygen uptake, $k_{p,tot}$, oxide growth, $k_{p,ox}$, and oxygen dissolution, $k_{p,sol}$

T (°C)	$k_{p,tot}$ ($10^4 mg^2 cm^{-4} h^{-1}$)	$k_{p,ox}$ ($10^4 mg^2 cm^{-4} h^{-1}$)	$k_{p,sol}$ ($10^4 mg^2 cm^{-4} h^{-1}$)
600	43	34	0.6
650	153	64	15
700	625	275	70

TABLE III Comparison between Ti6Al4V and various titanium alloys [9] of the amounts of oxygen dissolved in the metallic core during oxidation in air at 700 °C for 435 h

Alloy	O_{SOL} ($mg cm^{-2}$)	O_{SOL}/O_{TOT} (%)
Ti6Al4V	1.48[a]	27[a]
Ti cp	1.99	43
Ti1.65Al	2.02	44
Ti3Al	1.91	45
Ti5Al	1.06	49

[a] Values calculated after 300 h oxidation.

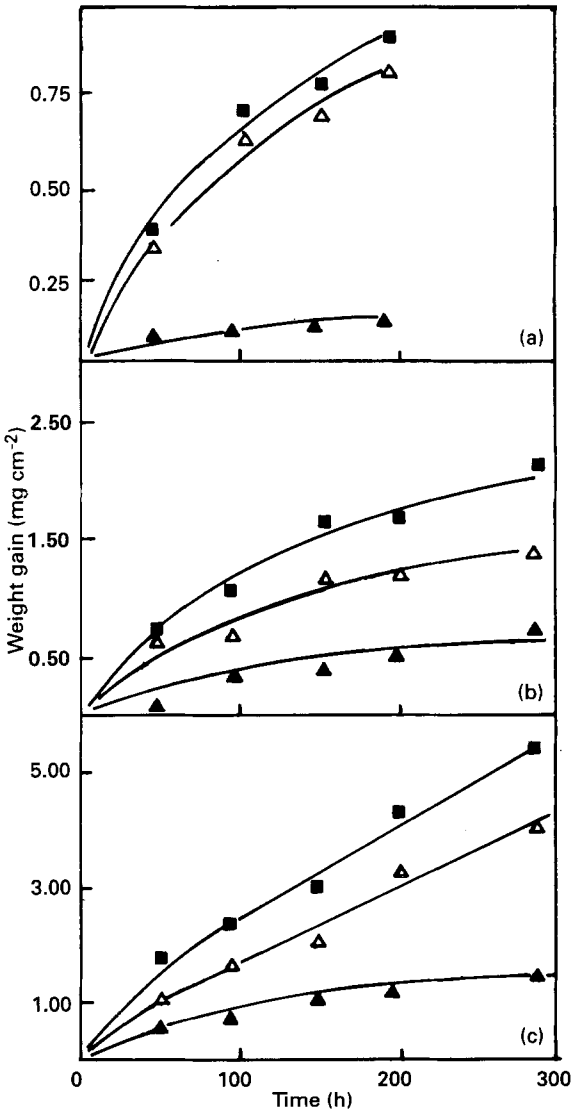

Figure 2 Influence of temperature on the kinetics of (△) scale growth and (▲) oxygen dissolution compared with (■) the total oxygen uptake at (a) 600 °C, (b) 650 °C, (c) 700 °C.

enabled the amount of oxygen dissolved in the metal to be calculated. The results are summarized in Fig. 2 and in Table II. Parabolic scale growth was found at 600 and 650 °C for the entirety of the exposure time range. At 700 °C, the scaling behaviour appeared to conform rather well with the shape of the overall weight-gain curve reflecting the same gradual transition from a nearly cubic to a linear kinetics. Conversely, the variation of oxygen dissolved in the alloy conformed always to a parabolic kinetics. From Fig. 2 it is also evident that the oxygen dissolution gives rise to an important contribution to the overall weight gain starting from 650 °C. This can be qualitatively predicted if one considers that the activation energy calculated for oxygen dissolution is much higher (340 kJ mol^{-1}) than for oxide growth (147 kJ mol^{-1}). Hence, the contribution of the dissolution process should increase with increasing temperature, at least until the overall kinetics remains parabolic. Thus, for example, the amount of oxygen in the alloy is seen ranging from about 10% at 600 °C to a maximum of 35% at 700 °C after 150 h. For longer times, the relative amount of oxygen in solid solution has been observed to decrease as a consequence of a reduced oxygen gradient caused by the onset of accelerated scale growth rate. In Table III, a comparison of the relative amounts of oxygen dissolved is made with literature data for various titanium alloys [9]. Thus, the influence of aluminium results in a marked reduction of the oxygen dissolved in the metal lattice, compared with unalloyed titanium and in agreement with the trend observed for binary Ti–Al alloys. On the other hand, the presence of vanadium should explain the strong reduction in the percentage of dissolved oxygen (compare the second row of Table III) with respect to the total oxygen uptake.

3.2. Oxygen diffusion in the metal surface layer

Microhardness profiles in the alpha-phase were measured in the alloy below the scale for different times in the range 600–700 °C. The results of the determinations are shown in Fig. 3. It is evident that the oxygen penetration distances increase with increasing time and/or temperature. For instance, the embrittled zone increases from 40 μm at 600 °C after 200 h to more than 80 μm at 700 °C after 300 h oxidation. However, coincident with the onset of accelerated oxide growth rate, the hardness gradients become less steep. At 650 °C this is observed between 200 and 300 h oxidation, whereas at 700 °C it occurs between 100 and 150 h.

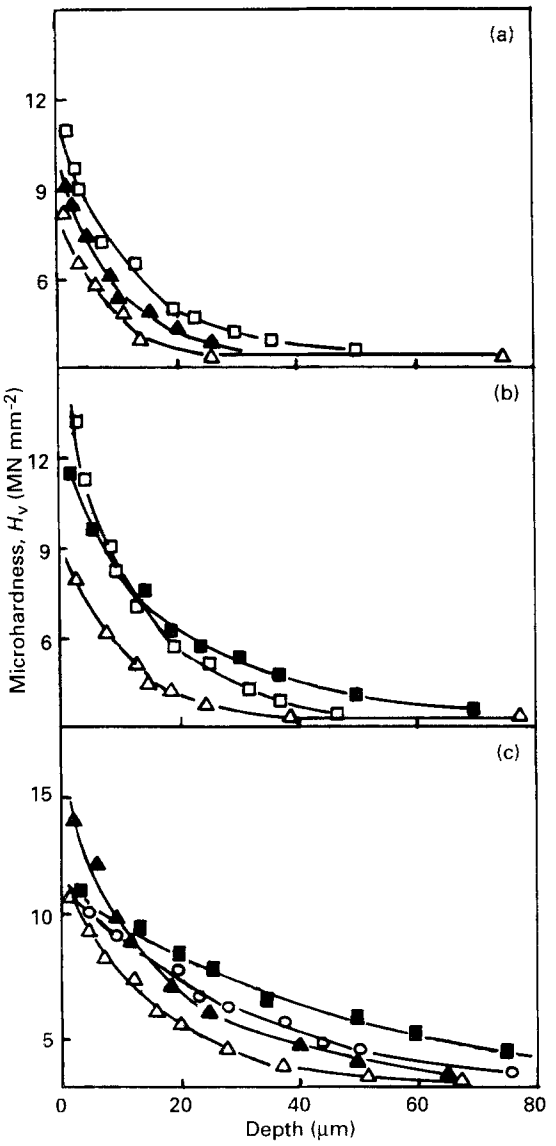

Figure 3 Evolution of the microhardness gradients in the metallic core as a function of temperature and oxidation time: (a) 600 °C, (b) 650 °C, (c) 700 °C; (△) 50 h, (▲) 100 h, (○) 150 h, (□) 200 h, (■) 300 h.

Approximative values for oxygen diffusion coefficients in the alpha-phase were also determined using the microhardness profiles after 100 h oxidation by assuming that oxygen concentration is proportional to its hardness [11]. For the case of growth of a protective surface scale with a concomitant oxygen dissolution in the metal substrate, Pemsler [15] has drawn the following analytical solution

$$\frac{C_x}{C_s} = \frac{\mathrm{erfc}(x'/2D^{1/2}t)}{\mathrm{erfc}(s/2D^{1/2}t)} \quad (1)$$

where C_s is the surface concentration, C_x is the concentration of diffusing oxygen at the distance x from the surface, s is the distance between the metal/oxide interface and the initial surface and $x' = x + s$; D denotes the diffusion coefficient in cm^2 s^{-1} when the distance x and the time t are expressed in cm and seconds, respectively. The position of the initial metal surface was calculated measuring the thickness of the scale and converting it to the corresponding thickness of metal consumed. To determine a reasonable value for s, use was made of the Pilling–Bedworth ratio for the TiO_2/Ti system.

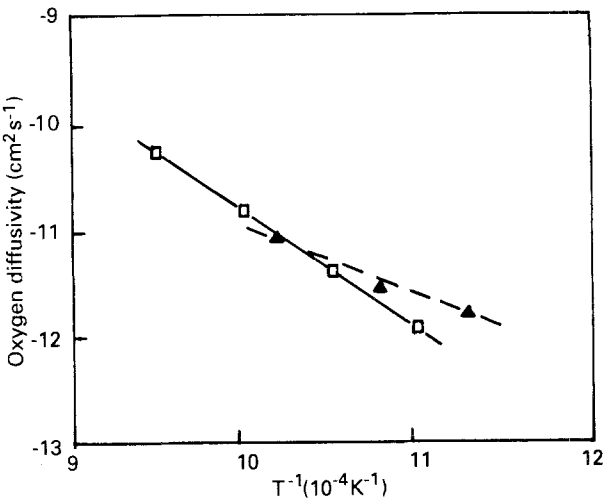

Figure 4 Arrhenius plot for the oxygen diffusion coefficient showing the comparison between (▲) Ti6Al4V and (□) pure titanium [14].

The diffusion coefficients were calculated point-by-point along the regression curves that were found to follow almost exactly an error function solution in agreement with Pemsler's model. The results are shown in Fig. 4 in Arrhenius form. These values are in good agreement with those determined for unalloyed titanium in similar conditions of oxidation [14].

3.3. Oxide scale characterization

The scale present on the surface of the Ti6Al4V after the oxidation tests gave X-ray diffraction patterns characteristic of the TiO_2 rutile phase. Weak diffraction signals correspondent to the Al_2O_3 phase were also found, but only on specimens oxidized at 700 °C. However, it is believed that alumina is present in intimate mixture with rutile also at lower temperatures. This opinion is consistent with the information obtained by EDX microanalysis. Quantitative spot measurements were made through polished cross-sections of oxide scales grown during oxidation at both 600 and 650 °C; the results are given in Fig. 5. The actual concentration profiles of the elements were calibrated using standards of their corresponding oxides. Bearing in mind the extremely low solubility of alumina in the rutile phase below 1000 °C [12], these concentration profiles of aluminium suggest strongly the presence of the alumina phase, at least in the outer part of the scale. In fact, EDX analysis indicates that there is a significant enrichment of the aluminium near the oxide/gas interface, which tends to increase with increasing temperature, although the concentration of aluminium in the alloy is not sufficient to promote the formation of a continuous film of alumina. These results are also in agreement with similar observations made for binary Ti–Al alloys [8, 9, 16]. For vanadium, because no oxidized phase was observed, it is highly likely that it would be present for the most part as VO_2 dissolved in the TiO_2 rutile phase. Another piece of information given by EDX is that the concentration of the aluminium in the oxide scale is higher than that which could be found if oxidation of the alloying elements had been taking place uniformly (see Table IV).

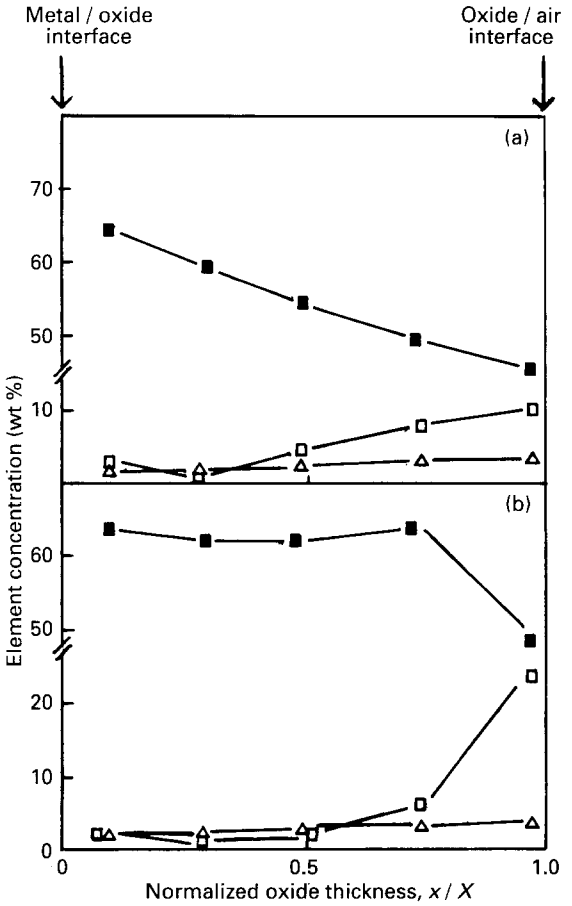

Figure 5 Concentration profiles of (■) titanium, (□) aluminium and (△) vanadium in the scale at (a) 600 and (b) 650 °C plotted against the normalized oxide thickness (x = distance from the alloy/oxide interface; X = total oxide thickness).

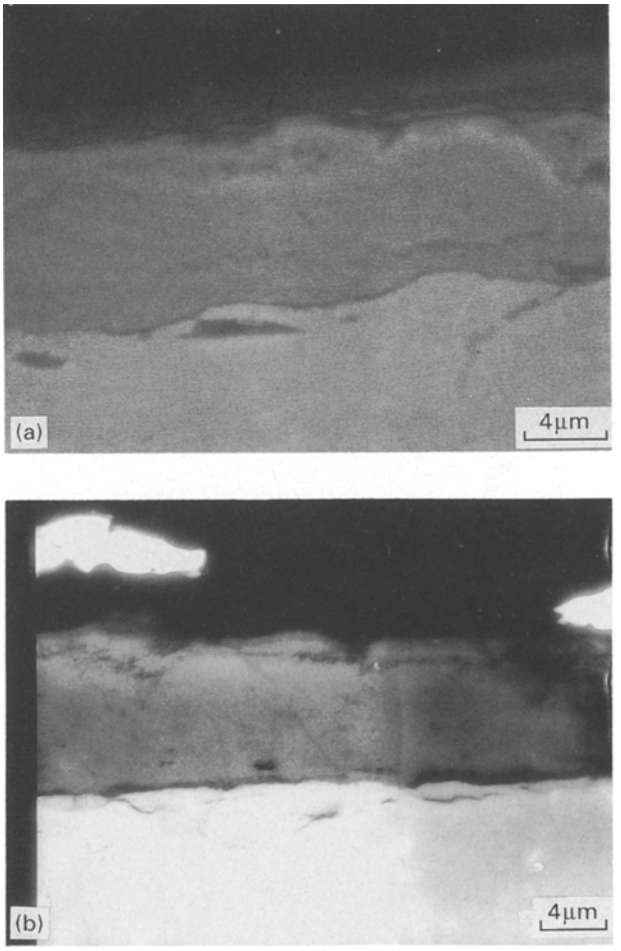

Figure 6 Metallographic cross-sections of oxide scales formed after 100 h exposure at (a) 600 °C and (b) 650 °C.

TABLE IV Hypothetical oxide composition (wt %) for the case of uniform oxidation compared with the actual composition of the oxide grown after 100 h at 600 °C, showing the enrichment of aluminium in the oxide

Element	Alloy composition	Oxide composition	Oxide composition in the case of uniform oxidation
Ti	88.9	53.7	52.7
Al	6.3	7.3	3.7
V	4.9	2.4	2.9

TABLE V Comparison of the parabolic rate constants, k_p, of Ti6Al4V with various titanium alloys

Alloy	k_p ($10^4 mg^2 cm^{-4} h^{-1}$)				Reference
	550 °C	600 °C	650 °C	700 °C	
Ti6Al4V	–	43	153	625	Present work
Ti6Al4V	–	29	150	1040	[10][a]
Ti cp	5.5	37	170	578	[9]
Ti1.65Al	1.0	12	–	–	[9]
Ti3Al	1.0	10	82	–	[9]
Ti5Al	0.7	7	54	–	[9]

[a] We have deduced the rate constants from the thermogravimetric curves presented in [10].

In order to obtain a better understanding of the film growth law, the morphology and structure of the scales have been carefully examined. Two different types of scale were observed. At 600 °C the oxidation gave a grey, dense and adherent film (Fig. 6a), which on metallographic examination appeared to be void-free. The observation of the surface scale gave no evidence of cracking even at the longest exposure time (Fig. 7a).

At 650 °C, the onset of a scale was noted, consisting of a layered structure with a strong tendency to spall off at the slightest contact, leaving uncovered a very thin but adherent inner layer. The development of the layered nature of the film was gradual and dependent on time. At 650 °C, the brittle part of the film appeared to develop as a duplex scale after prolonged exposure (Fig. 6b). The surface structure of the scales evinces the oxide grain imprints in the form of agglomeration of balls, between which fissures develop. These features are illustrated in Fig. 7b. Fractographic examination of the brittle scale indicates that the structure is usually coarser grained in the subsurface area and is somewhat finer grained at small distances from the inner interface. Voids are clearly visible and appear to be uniformly distributed throughout the scale. Sometimes, it is possible to distinguish between two layers (see Fig. 8).

The oxide film formed at 700 °C is quite similar to that observed on samples oxidized at 650 °C, except

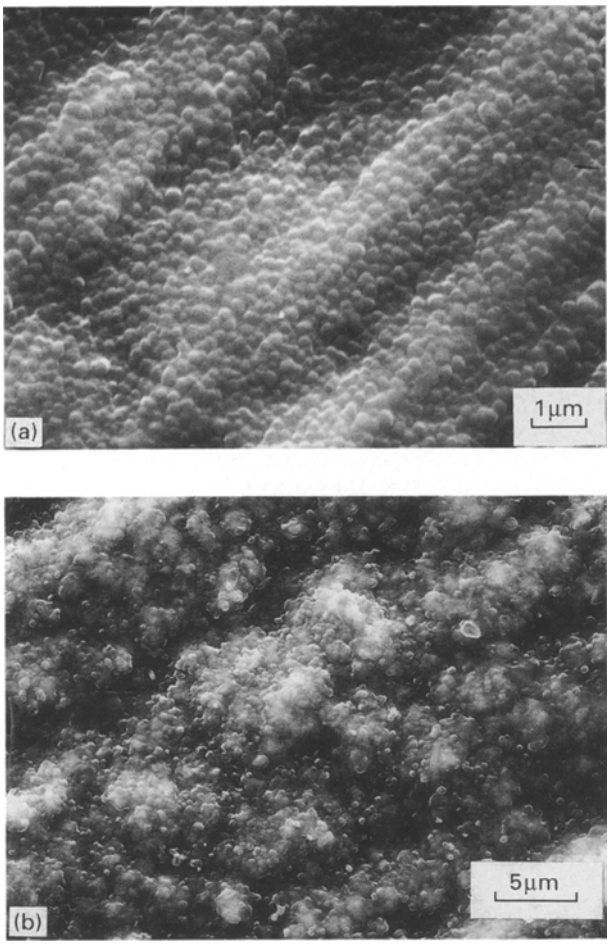

Figure 7 SEM images of the external oxide surfaces after 100 h oxidation at (a) 600 °C and (b) 650 °C.

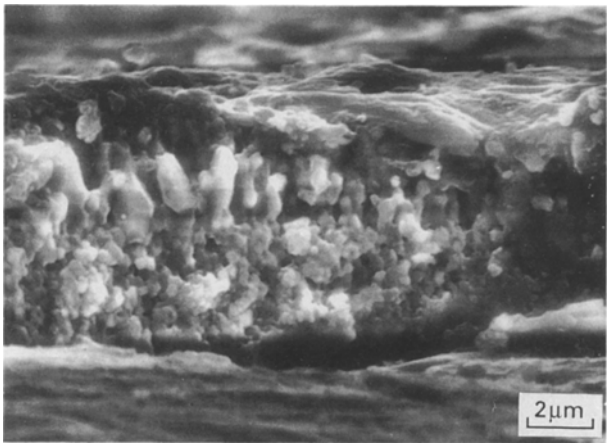

Figure 8 Scanning electron fractograph of the oxide scale formed after 150 h oxidation at 650 °C.

that the duplex nature of the scale is already evident even at the shortest exposure time (50 h).

4. Discussion

The results presented in the previous section have shown that the overall reaction kinetics exhibit a progressive transition, dependent both on time and temperature, from a nearly cubic to a linear oxidation rate. This is in good agreement with the earlier observations of Champin *et al.* [10], who reported similar results for Ti6Al4V oxidized in air. Table V compares some rate constants taken from the literature with the results of the present investigation. It appears that the oxidation rates of Ti6Al4V are more rapid than Ti–Al alloys containing 1.65%, 3% and 5% aluminium and comparable to unalloyed titanium, at least in this range of temperatures. In addition, the activation energy is similar to titanium. However, according to Champin *et al.* [10], at temperatures higher than 700 °C, the Ti6Al4V develops better protective properties than pure titanium, indicating that different rate-determining mechanisms become operative at higher temperatures. Analogous effects have been observed when oxidation was carried out in pure oxygen. For example, Sarrazin and Coddet [17] found that Ti6Al4V oxidizes more slowly than titanium in the temperature range 700–1000 °C.

Generally, aluminium is reported to have a beneficial role in reducing oxidation rates in binary titanium alloys also at the temperatures considered in this investigation (up to 700 °C). Depending on the aluminium content in the alloy, it is usually reported that the action of aluminium develops either in the decrease of the diffusion rate of oxygen in the oxide, caused by incorporation of trivalent aluminium ions in interstitial positions of the rutile lattice, or in a blocking effect due to the alumina particles finely dispersed in the rutile phase [9]. On the contrary, little information is available concerning the effect of vanadium, except that addition of vanadium to titanium leads to faster oxidation rates [10]. However, in our opinion, a reasonable explanation may be found in terms of the Wagner–Hauffe theory, considering the analogies existing with the behaviour of the rutile phase, $V_xTi_{1-x}O_2$ ($x \leqslant 0.1$), utilized as the catalyst active in oxidation reactions [18]. It has been observed that, although the solid solution stabilizes the reduced valence state of vanadium (V^{4+}), oxygen diffusion in the rutile phase may lead to localized oxidation of V^{4+} with consequent formation of either anion vacancies or interstitial cations. Under these conditions, limited amounts of V_2O_5 can also be formed [19]. Applying these considerations to a growing oxide film, it is reasonable to expect an increase in the oxidation rate, if the anion vacancies are predominant. This effect is indeed observed experimentally when vanadium is added to titanium. For the mechanisms related to the observed change in the oxidation rate equation between 600 and 700 °C, evidence has been presented that oxygen dissolution in the alloy always obeys a diffusive kinetics in this temperature range. Moreover, in comparison to unalloyed titanium, the presence of aluminium and vanadium leads to a decrease in the importance of the oxygen dissolved in the alloy substrate. Thus, it is not surprising that the passage to an unprotective overall oxidation rate reflects mainly an acceleration of the scale growth rate. Because this phenomenon has been observed to proceed with the development of a layered character of the scale, it is reasonable to associate these two aspects. Thus, it is possible that the transition to a linear oxidation might arise from a process controlled by diffusion through a barrier of fixed dimensions,

which could be the very thin inner layer. A similar explanation has been proposed by Jenkins for unalloyed titanium [20]. Unfortunately, we were unable to determine with accuracy the thicknesses of the inner layer in order to support this hypothesis.

5. Conclusions

The air oxidation behaviour of the ternary Ti6Al4V alloy has been studied in the temperature range 600–700 °C. The following main conclusions are drawn.

1. The alloy oxidizes at rates comparable to unalloyed titanium, exhibiting a progressive transition dependent both on time and temperature from a diffusion-controlled to a nearly linear rate law. Considering the short time scale of the oxidation tests, the time dependence is clearly seen only at 700 °C, where a unique value of the rate exponent is inadequate to describe the oxidation process at both short and long times.

2. The reaction kinetics for both oxide scale growth and oxygen dissolution in the alloy surface layer have been determined. This latter process always conforms to a parabolic rate equation, whereas the shape of the scale growth curve is similar to the overall kinetic curve. This means that the transformation to a linear oxidation is sustained mainly by an accelerated scale growth rate.

3. This acceleration in the oxide film growth is accompanied by a correspondent change in the morphology of the scale. Microscopic examination indicates the onset of a duplex nature starting from 650 °C, which becomes more and more pronounced as a function of time and temperature.

4. From microhardness gradients, the penetration distances of the oxygen in the alloy have been calculated in order to establish the extent of the embrittled zones. Finally, oxygen diffusion coefficients in the alloy have been determined. They were found to be quite similar to those reported for unalloyed titanium under analogous oxidation conditions.

Acknowledgements

The authors thank the technical staff who collaborated at this investigation: Mr G. Cigna for carrying out the oxidation experiments, Mr T. Carmeni for preparation of metallographic samples, Mr A. Masci for work on the scanning electron microscope and Mr A. Di Bartolomeo for the X-ray diffraction analysis.

References

1. A. KHATAEE, H. M. FLOWER and D. R. F. WEST, *J. Mater. Eng.* **10** (1988) 37.
2. P. L. MARTIN, M. MENDIRATTA and H. A. LIPSITT, *Metall. Trans.* **14A** (1983) 2170.
3. W. J. S. YANG, *ibid.* **13A** (1982) 324.
4. C. E. SHAMBEN and T. K. REDDEN, "Science and Technology and Application of Titanium", R. I. Jaffee and N. E. Promisel eds. (Pergamon, Oxford, 1966) p. 199.
5. D. J. LAINER, E. N. SLESAREVA, M. J. TSIPIN and A. S. BAI, *Zashch. Met. (USSR)* **2** (1966) 692.
6. V. M. POPOVA, Z. I. KORNILOVA and E. M. LAZAREV, *ibid.* **10** (1974) 345.
7. I. A. MENZIES and K. N. STRAFFORD, in "Proceedings of the 3rd International Congress on Corrosion of Metals", Vol. 4 (Mir, Moscow, 1968) p. 93.
8. A. M. CHAZE, C. CODDET and G. BERANGER, *J. Less-Common Metals* **83** (1982) 49.
9. A. M. CHAZE and C. CODDET, *ibid.* **157** (1990) 55.
10. B. CHAMPIN, L. GRAFF, M. ARMAND, G. BERANGER and C. CODDET, *ibid.* **69** (1980) 163.
11. A. M. CHAZE and C. CODDET, *J. Mater. Sci.* **22** (1987) 1206.
12. G. WELSH and A. I. KAHVECI, in "Proceedings of the Workshop on Oxidation of High-Temperature Intermetallics", Cleveland, OH, 22–23 September 1988, T. Grobstein and J. Duychak eds. (The Minerals, Metals and Materials Society, Warrendale, PA, 1989) p. 207.
13. G. H. MEIER and D. APOLLONIA, *ibid.* p. 185.
14. D. DAVID, E. A. GARCIA, X. LUCAS and G. BERANGER, *J. Less-Common Metals* **65** (1979) 51.
15. J. P. PEMSLER, *J. Nucl. Mater.* **7** (1962) 16.
16. A. M. CHAZE and C. CODDET, *J. Less-Common Metals* **124** (1986) 73.
17. P. SARRAZIN and C. CODDET, *Corros. Sci.* **14** (1974) 83.
18. A. ANDERSSON and S. L. T. ANDERSSON, in "Solid State Chemistry in Catalysis", R. K. Grasselli and J. F. Brazdil, eds. (American Chemical Society Symposium Series 279 Washington, DC, 1983) p. 121.
19. H. KUNG, in "Transition Metal Oxides: Surface Chemistry and Catalysis", edited by B. Delmon and J. T. Yates (Elsevier, Amsterdam, 1989) p. 12.
20. A. E. JENKINS, *J. Inst. Metals.* **82** (1953–54) 213.

Received 7 September 1992
and accepted 20 August 1993